In Vivo Degradation Behavior of Photo-Cross-Linked *star*-Poly(ϵ-caprolactone-*co*-D,L-lactide) Elastomers

Brian G. Amsden,*,† M. Yat Tse,‡ Norma D. Turner,† Darryl K. Knight,† and Stephen C. Pang‡

Departments of Chemical Engineering and of Cell Biology and Anatomy, Queen's University, Kingston, Ontario, Canada K7L 3N6

Received September 29, 2005

We have recently reported on the preparation of biodegradable elastomers through photo-cross-linking acrylated *star*-poly(ϵ-caprolactone-*co*-D,L-lactide). In this paper we assess the change in their physical properties during in vivo degradation in rats after subcutaneous implantation over a 12 week period. These parameter changes were compared to those observed in vitro. Two different cross-link densities were examined, representing the range from a high Young's modulus to a low Young modulus. Elastomers having a high cross-link density exhibited degradation behavior consistent with a surface erosion mechanism, and degraded at the same rate in vivo as observed in vitro. Young's modulus and the stress at break of these elastomers decreased linearly with the degradation time, while the strain at break decreased slowly. Elastomers having a low cross-link density exhibited a degradation mechanism consistent with bulk erosion. Young's modulus and the stress at break of these elastomers decreased slowly initially, followed by a marked increase in mechanical strength loss after 4 weeks. The elastomers were well tolerated by the rats over the 12 week period in vivo.

Introduction

Synthetic, biodegradable elastomers based on aliphatic polyesters have a number of potential biomaterial applications, including as scaffolds for engineering soft tissue[1−7] and as drug delivery depots.[8−11] These materials are particularly suitable for situations where biomaterial mechanical properties should more closely mimic the extracellular matrix for tissue engineering or biocompatibility reasons. A number of biodegradable elastomers have been developed, which can be divided into thermoplastics[5,12−22] and thermosets.[10,23−28] Thermoplastics, due to their semicrystalline nature, often degrade in a heterogeneous manner, with the amorphous regions degrading faster than the crystalline regions, because of the ease of water penetration into the amorphous regions. This degradation behavior can be disadvantageous because it produces a nonlinear strength loss with respect to mass loss with time, and often total mechanical failure before a significant mass loss has occurred.[29] In that respect, amorphous thermosets can be viewed as possessing more desirable degradation properties.

We have recently reported on the preparation and in vitro characterization of elastomers prepared from photo-cross-linking an acrylated *star*-poly(ϵ-caprolactone-*co*-D,L-lactide) macromonomer using UV or visible light,[30] and demonstrated the possibility of obtaining nearly zeroth-order in vitro release of interferon-γ delivered from a biodegradable, photo-cross-linked elastomer, while maintaining a very high degree of protein bioactivity during the release period.[31] In this approach, the protein is distributed as a solid, colyophilized with a highly osmotic excipient, throughout the elastomer matrix. The protein is released through the use of an osmotic-pressure-driven release mechanism, generated by the excipient. The release rate is determined to a large extent by the mechanical properties of the elastomer. As a natural progression in the development of the elastomer delivery vehicle, it is necessary to determine the changes in its mechanical properties with time during in vivo biodegradation as well as its in vivo biocompatibility. Furthermore, it would be useful to be able to compare these changes to those observed in vitro as a means of developing a rapid screening technique for device development.

Polyesters are considered to degrade in vivo primarily by bulk hydrolysis.[32] Various groups have shown that degradation occurs at a faster rate in vivo than in vitro. For example, Therin et al.[33] found that PLGA 2 mm thick disks degraded at a faster rate when implanted subcutaneously in sheep than when degraded in phosphate buffer maintained at body temperature. Moreover, this degradation behavior was not strongly geometry dependent as it has been reported that PLGA microspheres also degrade faster in vivo than in vitro.[34−36] Similar findings of greater degradation in vivo than in vitro have been reported for PLGA ligating clips.[37] The same behavior occurs for other aliphatic polyester polymers and copolymers. Poly(lactide) formed into rods,[38,39] spinal cages,[40] and screws and plates[41] has been reported to lose mass faster in vivo than in vitro. Jeong et al. have recently reported that random, equimolar monomer composition, thermoplastic copolymers of caprolactone and L-lactide fashioned into 2 mm diameter rods lost mass faster in vivo than in vitro.[42] The faster in vivo degradation has been attributed to plasticization of the polymer due to the absorption of lipids or other biological compounds, leading to greater water uptake, the foreign body response, the action of enzymes, a greater solubility of the degradation products in vivo, and the influence of additional mechanical stresses experienced in vivo.[25,35,43−45]

There are fewer reports concerning the change in mechanical properties of aliphatic polyesters with degradation in vitro versus in vivo. The evidence thus far indicates that the mechanical properties of un-cross-linked aliphatic polyesters decrease at the same rates in vivo as observed in vitro. For example, Weir et

* To whom correspondence should be addressed.
† Department of Chemical Engineering.
‡ Department of Cell Biology and Anatomy.

10.1021/bm050731x CCC: $33.50
Published on Web 11/15/2005

al.[46] examined the in vitro versus in vivo degradation of poly(L-lactide) (2 mm rods implanted subcutaneously in rats) and found that the shear strength of the rods changed at the same rate in vitro as in vivo. Mainil-Varlet et al.[38] found that the bending modulus, bending strength, and shear strength of 3.2 mm poly(D,L-lactide) bars implanted subcutaneously into sheep decreased at the same rate in vitro as in vivo. Additionally, Saikku-Backstrom et al.[47] found that self-reinforced fibrillated poly(96L/4D-lactide) rods lost mechanical strength at statistically identical rates in vitro and in vivo. These results are contrary to the findings of Suuronen et al.,[41] who found that the mechanical strength of self-reinforced poly(L-lactide) screws and multilayer plates degraded faster in vivo than in vitro; however, this was attributed to the greater mechanical stresses experienced by the screws and plates in vivo than in vitro.

Although there are reports on the in vitro degradation of photocured[30,48,49] and thermocured[23,29,50] aliphatic polyester elastomers, there have been comparatively few reports on the in vivo degradation of cured aliphatic polyester elastomers. For the one elastomer that has been reported, Pitt and co-workers[25,45] have reported on the in vitro versus in vivo degradation of poly(ϵ-caprolactone-*co*-δ-valerolactone) cross-linked with varying amounts of bis(ϵ-caprolacton-4-yl)propane added to the monomers during polymerization. These thermally cured elastomers showed little mass loss in vitro, but in vivo exhibited a linear mass loss. The increase in and character of the in vivo degradation rate were taken as evidence of enzymatic degradation. In contrast, the mechanical properties decreased at the same rate during in vitro or in vivo degradation. Moreover, mass loss in vivo occurred in a zeroth-order fashion and increased as the cross-link density of the elastomers decreased.

It is the objective of this paper to examine the influence of cross-link density on the in vivo change in physical and mechanical properties of a photo-cross-linked elastomer based on acrylated *star*-poly(ϵ-caprolactone-*co*-D,L-lactide) and compare this degradation behavior to that which occurs in vitro. The elastomers prepared from this macromonomer have an architecture and monomer composition different from those of the elastomers prepared by Pitt and colleagues, and photo-cross-linking results in the generation of oligo(acrylate) regions. Each of these factors produces degradation characteristics different from those observed previously. Two cross-link densities representing a tightly cross-linked elastomer having a high Young modulus and a loosely cross-linked elastomer possessing a relatively low Young modulus are compared.

Materials and Methods

D,L-Lactide (99+%) was obtained from Purac (The Netherlands) and purified by recrystallization from toluene immediately prior to use. ϵ-Caprolactone was obtained from Lancaster (Canada), dried over CaH_2 (Aldrich, Canada), and distilled under nitrogen. Other chemicals used in the synthesis of the star copolymer macromonomers were stannous 2-ethylhexanoate (96%) (Aldrich, Canada) and glycerol (99.5%) (BDH). The chemicals used in the synthesis of the acrylated star copolymers include acryloyl chloride (96%), triethylamine (99.5%), and 4-(dimethylamino)pyridine (99%), all obtained from Aldrich, Canada. Other chemicals used include anhydrous dichloromethane (99.9%) and ethyl acetate (99.9%) obtained from Fisher, Canada. The long-wave UV initiator 2,2-dimethoxy-2-phenylacetophenone (99%) was obtained from Aldrich, Canada.

Preparation of Elastomers. The method of preparation and characterization of the elastomers were as described previously.[30] Briefly, *star*-poly(ϵ-caprolactone), *star*-poly(D,L-lactide), and *star*-poly(ϵ-caprolactone-*co*-D,L-lactide) of equimolar caprolactone:lactide composition were prepared through melt ring-opening polymerization initiated by glycerol and catalyzed with stannous 2-ethylhexanoate (140 °C for 24 h). The star homopolymers were purified by precipitation from tetrahydrofuran into water and then dried completely under mild heat and vacuum in the presence of desiccant, while the star copolymers were purified by extracting the polymer with methanol for 2 h at −20 °C. The extraction process was repeated twice. Overall yields of acrylated star polymer were 80−85 mass %.

Two molecular weights were chosen for examination: 1250 and 7800. These star copolymers were converted to telechelic macromonomers by reaction of the terminal hydroxyl groups with acryloyl chloride, catalyzed with 4-(dimethylamino)pyridine while triethylamine was utilized as a HCl scavenger. Proton nuclear magnetic resonance (^{1}H NMR) spectroscopy was used to confirm the lactide:caprolactone monomer ratio and that a random star copolymer was formed, and to determine the degree of acrylation. ^{1}H NMR was performed in both $CDCL_3$ and d_6-DMSO using a Bruker Avance-600 NMR spectrometer. Chemical shifts were measured relative to the methyl proton resonance of internal tetramethylsilane. The molecular weights of the telechelic macromonomers were confirmed using a Waters Alliance GPC system connected to a Wyatt Dawn EOS multiangle laser light scattering (MALLS) detector. The mobile phase consisted of THF at a flow rate of 1 mL/min with the system at 35 °C. The concentration of the polymers used for the GPC measurements was 30 mg/mL, and the injection volume was 50 μL. The column configuration consisted of an HP Phenogel guard column attached to a Phenogel linear (2) 5 μm GPC column. The increment of refractive index used in molecular weight calculations was measured using a Wyatt Optilab refractometer and found to be 0.064 mL/g.

The macromonomers were photopolymerized by first dissolving the telechelic macronomomers in THF at a ratio of 1 g of macromonomer to 1 mL of THF. To this solution was added 0.015 mg of 2,2-dimethoxy-2-phenylacetophenone as the UV photoinitiator per milligram of telechelic macromonomer. This solution was poured into 2.5 mm inside diameter glass tubing that had been flame dried and sealed at one end. The tubing was then sealed at the open end using Parafilm and subjected to 20 mW/cm^2 long-wave UV irradiation (320−480 nm) for 3 min using an EXFO E3000 high-intensity long-wave lamp. The Parafilm was removed and the THF allowed to slowly evaporate for 24 h. Note that short-wave UV irradiation could have been used; however, we are interested in incorporating protein drugs into these elastomers, and radiation of that energy would likely denature proteins. The elastomer cylinders thus prepared had a diameter of 1.8−2.0 mm, and were cut into 1 cm lengths. The sol portion of the elastomers (approximately 5 wt %[30]) was removed by immersion in THF. The cylinders were then soaked in ethanol, allowed to dry in a laminar flow hood, and stored in sterilized glass vials.

Subcutaneous Implantation in Rats. Adult male Wistar rats (Charles River Laboratories, Quebec, Canada) weighing 250 g were anesthetized with 2% isoflurane (Baxter Corp.) in oxygen by inhalation via an Engler ADS 1000 (Benson Medical Industries) at a total flow rate of 0.2 mL/min of O_2. At a level of surgical anesthesia (i.e., lack of tail and corneal reflexes), the rats were shaved at the nape region. This site was chosen to minimize the possibility of rats chewing on the implant site postoperatively. Implantation surgery was done under aseptic conditions. The shaved area was disinfected with Hibitane, and four 1 cm longitudinal incisions were made to allow the implantation of four 1 cm cylindrical pieces of polymeric materials. Three segments of each polymeric formulation and one piece of 4-O metric Vicryl (Ethicon; as control) suture were implanted per rat. Following implantation, skin incisions were closed with silk suture. At 1, 2, 4, 8, and 12 weeks following implantation, the rats were anesthetized with an ip injection of Somnotol (60 mg/kg), and at a level of surgical anesthesia, the rats were shaved and polymers excised with the surrounding skin. Two of the polymer pieces were retrieved for mechanical and chemical measurements, and the third was fixed in 4% paraformaldehyde in phosphate-buffered saline, processed for paraffin embedding, and

stained with hematoxylin and eosin for routine histological examination. These studies were done under the guidelines of the code of ethics governing animal experimentation.

Physical Measurements of Explanted Cylinders. Immediately after explantation, the elastomer cylinders were weighed and measured. The mechanical properties of the freshly explanted elastomers were measured in uniaxial tension using an Instron uniaxial tensile tester, model 4443. The crosshead speed was set at 500 mm/min according to ASTM D412. All specimens were tested at room temperature. Data analysis was carried out using a Merlin 4.11 Series IX software package. The explants were then dried under vacuum at room temperature in the presence of desiccant for 48 h, and the dried mass was recorded. The sol content of the dried explants was determined with a Soxhlet apparatus using dichloromethane at 45 °C.

In Vitro Degradation. Elastomer cylinder samples were immersed in 15 mL of phosphate-buffered saline (PBS), pH 7.4 and 37 °C, in a 20 mL scintillation vial. Three samples for every time point were used. The buffer was replaced at weekly intervals. At each sampling time point, the cylinders were removed, blotted dry, weighed, and measured. The slabs were then subjected to a uniaxial tensile measurement while hydrated. The pieces from the tensile measurement were collected and dried under mild heat in a vacuum oven in the presence of desiccant for 1 week. The dried mass was then measured.

Results and Discussion

In the following discussion, the abbreviation SCP will refer to the star copolymer while the number following this abbreviation will refer to its molecular weight, and ELAST will refer to the elastomer prepared from the acrylated star copolymer (ASCP) while the number following this abbreviation will refer to the molecular weight of the ASCP used to prepare the elastomer. For example, ELAST 1250 refers to the elastomer prepared using an ASCP of molecular weight of 1250.

Characterization of the Macromonomer. The composition of the star copolymers, and their degree of acrylation, was determined via ^{1}H NMR. To aid in the determination of the proton peaks, low molecular weight (1250) *star*-poly(ϵ-caprolactone) and *star*-poly(D,L-lactide) were synthesized. It has been reported that the polymerization of ϵ-caprolactone with glycerol as initiator to prepare star polymers results in incomplete reaction of the glycerol hydroxyls at low monomer to initiator molar ratios,[51] and thus, it was necessary to determine whether incomplete conversion of the glycerol hydroxyls occurred with the star copolymer macromonomers used in this study. Low molecular weight (1250) *star*-poly(ϵ-caprolactone) and *star*-poly(D,L-lactide) were therefore characterized initially via ^{1}H NMR using $CDCl_3$ as the solvent. $CDCl_3$ was used so that comparisons could be made between the NMR spectra of these polymers and those of pure di- and triglycerides (1,2-dipalmitin, 1,3-dipalmitin, and tripalmitin) reported in the literature.[52] The ^{1}H NMR spectrum for *star*-poly(ϵ-caprolactone) is given in Figure 1, while the proton assignations of the possible polymer structures are given in Chart 1. The proton assignments in Figure 1 were confirmed using 2-dimensional ^{1}H NMR (COSY). The spectrum clearly shows the presence of 1,3- and 1,2-poly(ϵ-caprolactone)-disubstituted glycerol. However, the peaks attributed to 1,3-poly(ϵ-caprolactone)-disubstituted glycerol were significantly overlapped with peaks attributed to the glycerol CH_2 protons of 1,2-poly(ϵ-caprolactone)-disubstituted glycerol and *star*-poly(ϵ-caprolactone). For this reason, further spectra were obtained using d_6-DMSO as the solvent (Figures 2 and 3). Using d_6-DMSO provided higher spectral resolution of the glycerol peaks. The other advantage of using d_6-DMSO was that the hydroxyl peaks were available to use to determine the degree of acrylation of the functionalized macromonomers. Again, peak assignments were confirmed using 2-dimensional ^{1}H NMR (COSY).

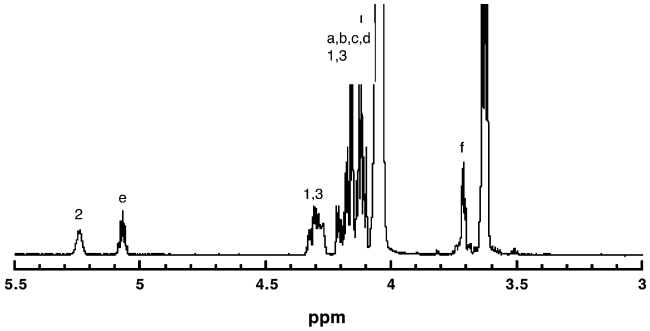

Figure 1. ^{1}H NMR spectrum of the glycerol portion of molecular weight 1250 *star*-poly(ϵ-caprolactone) in $CDCl_3$ solution. Peak assignments refer to protons labeled in Chart 1.

Chart 1. Possible Oligomer Structures with ^{1}H NMR Proton Assignations[a]

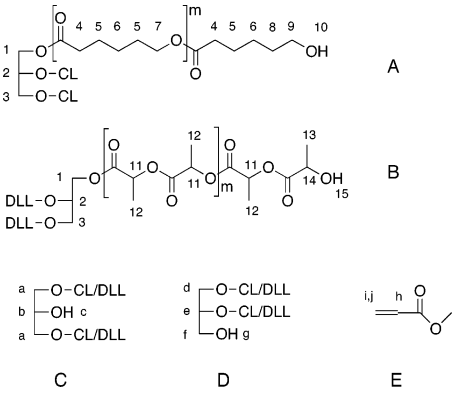

[a] For ^{1}H NMR proton assignments, see Figures 1−3. CL refers to a caproyl sequence, and DLL refers to a lactyl sequence. Key: (A) *star*-oligo(ϵ-caprolactone), (B) *star*-oligo(D,L-lactide), (C) 1,3-disubstituted glycerol, (D) 1,2-disubstituted glycerol, (E) terminal acrylate.

Analysis of the NMR spectra leads to the following observations. First, each SCP had approximately the same D,L-lactide content as far as can be determined using ^{1}H NMR, with the SCP 1250 being 51 mol % D,L-lactide, while the SCP 7800 contained 48 mol % D,L-lactide. A comparison of peak integrations attributed to glycerol peaks of the homo star polymers indicates that ϵ-caprolactone does not react as readily with glycerol as does D,L-lactide. The *star*-poly(ϵ-caprolactone) product was only 23 mol % three-armed star polymer (i.e., all the glycerol hydroxyls had been consumed to form a polymer chain), with the remainder being predominantly 1,3-poly(ϵ-caprolactone)-disubstituted glycerol (50 mol %) (Figure 2B), while the *star*-poly(D,L-lactide) product was 66 mol % three-armed star polymer and only 22 mol % 1,3-poly(D,L-lactide)-disubstituted glycerol (Figure 2A). This difference can be attributed to the higher reactivity of D,L-lactide.[53−55] The SCP 1250 product consisted of 85 mol % three-armed star copolymer and only 11 mol % 1,3-disubstituted glycerol (Figure 2C), while the SCP 7800 was completely three-armed star copolymer (Figure 3A). These results are similar to the findings of Lang et al.,[51] who observed that the consumption of the glycerol hydroxyl groups in the polymerization of ϵ-caprolactone was incomplete at low monomer to hydroxyl ratios, while at higher monomer to hydroxyl ratios all the glycerol hydroxyl groups had initiated a chain in the star polymer.

The average caproyl sequence length of the star copolymers can be determined by comparison of the peak areas centered at

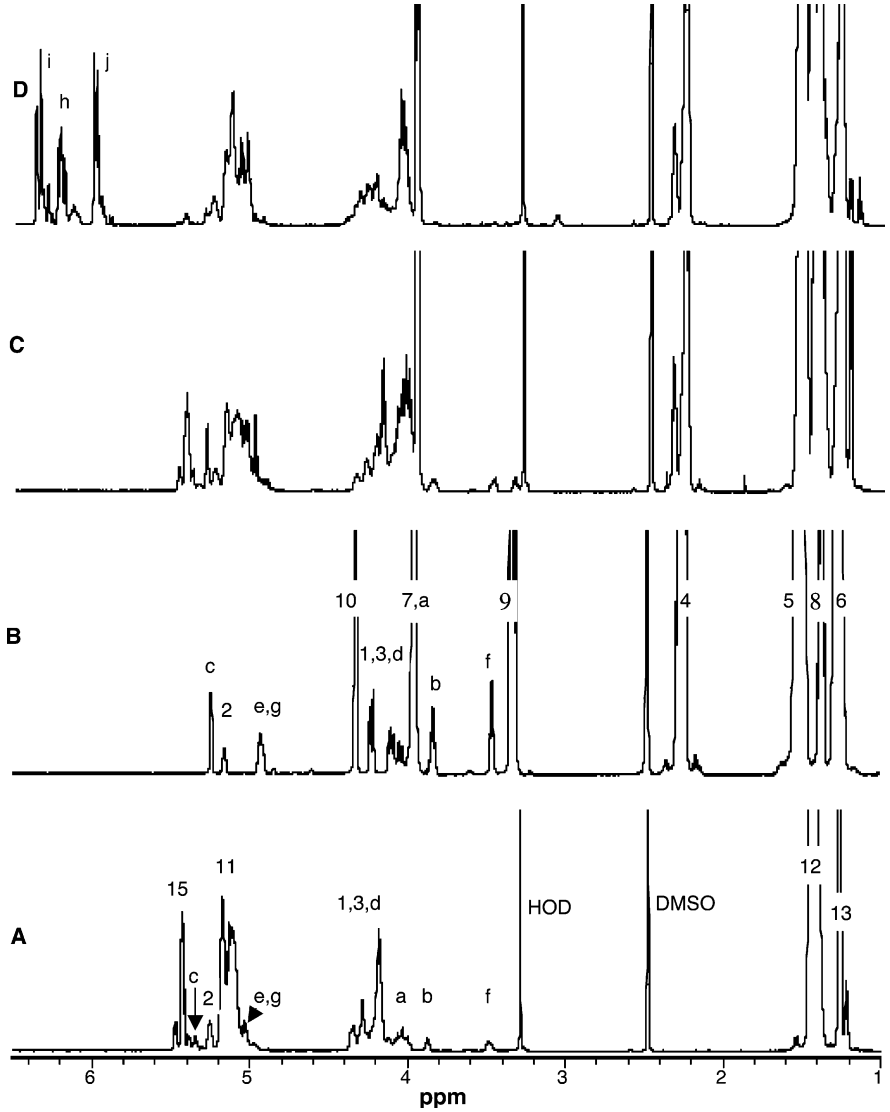

Figure 2. Stacked ^{1}H NMR spectra of molecular weight 1250 star polymers in d_6-DMSO solution. Peak assignments refer to protons labeled in Chart 1. Key: (A) *star*-poly(D,L-lactide), (B) *star*-poly(ϵ-caprolactone), (C) *star*-poly(ϵ-caprolactone-*co*-D,L-lactide), (D) terminus-acrylated *star*-poly(ϵ-caprolactone-*co*-D,L-lactide).

2.5 ppm, representing caproyl−caproyl sequences, and at 3.2 ppm, representing caproyl−lactyl sequences.[56] The average lactyl sequence length requires good peak separation in the 4.9−5.2 ppm region, as well as in the 3.9−4.1 ppm region. Good peak separation in these regions is clearly visible in the spectrum for SCP 7800 (Figure 3A); however, it was not possible to obtain good peak separation for SCP 1250, even with manipulation of the temperature. Therefore, only the average caproyl sequence length of the star copolymers can be compared. This comparison shows that SCP 1250 possesses a more blocky structure, with an average caproyl sequence length of 4.1, than does SCP 7800, which has an average caproyl sequence length of 2.3 and thus possesses a more random monomer distribution. Moreover, a caproyl sequence length of 4.1 for SCP 1250 indicates that some arms predominantly or totally consisted of ϵ-caprolactone, while others were predominantly D,L-lactide in composition.

The degree of functionalization of the hydroxyl end groups via esterification with acryloyl chloride is readily followed through the reduction in the peak intensities of the hydroxyl groups, at 4.33 ppm (caprolactone-terminated), 5.29 and 5.42 ppm (D,L-lactide-terminated), 5.25 ppm (unreacted glycerol hydroxyl on 1,3-disubstituted polymer), and 5.44 ppm (unreacted glycerol hydroxyl on 1,2-disubstituted polymer) present in Figures 2C and 3A. Figures 2D and 3B show the ^{1}H NMR spectra of the acrylated star copolymers, wherein these peaks are greatly reduced in intensity. The degree of acrylation for ASCP 1250, determined by a comparison of the decrease in the cumulative hydroxyl peak areas relative to the CH_3 peak areas of the D,L-lactide component, was 89%, while that of ASCP 7800 was 86%. Moreover, although SCP 1250 contained 1,3- and 1,2-disubstituted polymer fractions, the acrylated star copolymer was still trifunctional, as the glycerol hydroxyls left unconsumed during polymerization were readily acrylated. Thus, once cross-linked, the elastomers prepared from these functionalized macromonomers would have the same cross-link network functionality.

These two different ASCPs were used to prepare elastomer samples for implantation. The physical properties of these elastomers are given in Table 1. These elastomers represent the range from a high Young modulus (ELAST 1250) to a low Young modulus (ELAST 7800), i.e., a highly cross-linked network (ELAST 1250) and a more loosely cross-linked network (ELAST 7800)

Implantation Results. All of the rats gained weight and were active and healthy prior to implant removal. The implants were encapsulated with a fibrous tissue, visible at week 1 and

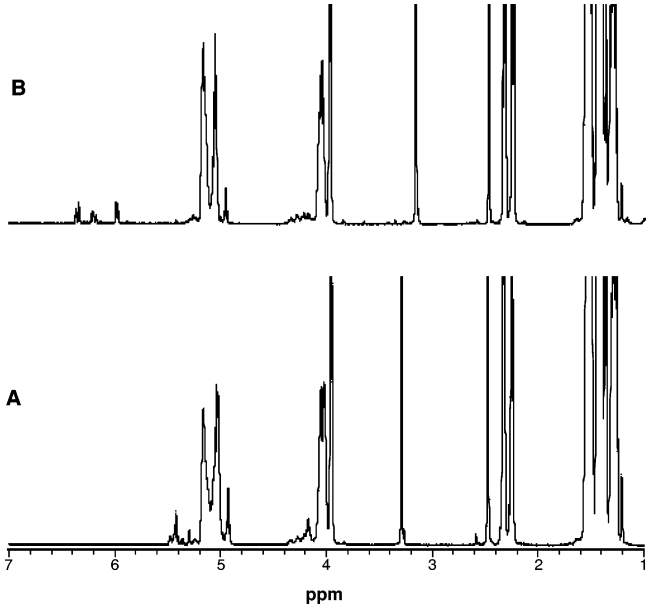

Figure 3. Stacked ^{1}H NMR spectra of molecular weight 7800 star polymers in d_6-DMSO solution. Peak assignments refer to protons labeled in Chart 1. Key: (A) *star*-poly(ϵ-caprolactone-*co*-D,L-lactide), (B) terminus-acrylated *star*-poly(ϵ-caprolactone-*co*-D,L-lactide).

Table 1. Glass Transition Temperature, T_g, Young's Modulus, E, Stress at Break, σ, and Strain at Break, ϵ, of the Elastomers As Prepared

elastomer	T_g (°C)	E (MPa)	σ (MPa)	ϵ (mm/mm)
ELAST1250	−2	5.3 ± 0.02	4.4 ± 0.02	0.79 ± 0.015
ELAST7800	−4	0.59 ± 0.13	1.7 ± 0.08	5.3 ± 0.23

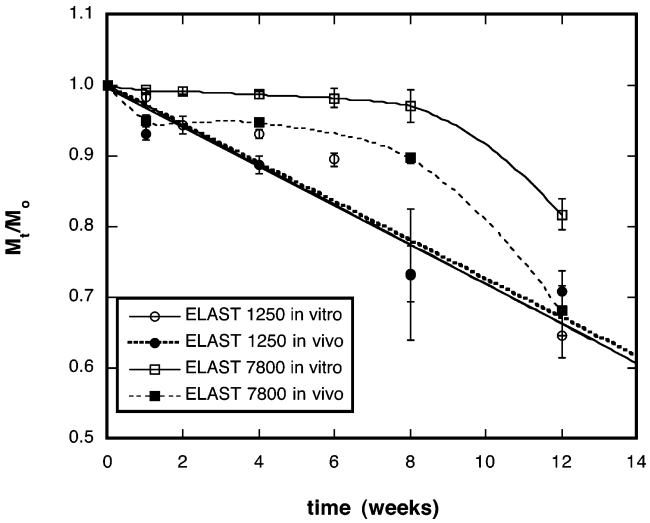

Figure 4. In vivo versus in vitro mass loss comparison for elastomers prepared using differing telechelic macromonomer molecular weight.

increasing in thickness until week 4, reaching a thickness of 80 ± 10 μm. The mass loss of the elastomers with degradation time both in vivo and in vitro is given in Figure 4 as a ratio of dry mass at time t, M_t, to initial dry mass, M_o. The rate of mass loss was dependent on the cross-link density, reflected in the molecular weight of the ASCP used to prepare the elastomer. The lower the molecular weight of the ASCP, the greater the cross-link density of the elastomer.[30] Both elastomers experienced a marked increase in degradation in vivo compared to that observed in vitro over the first week of implantation. This result is likely due to the acute inflammatory response in vivo

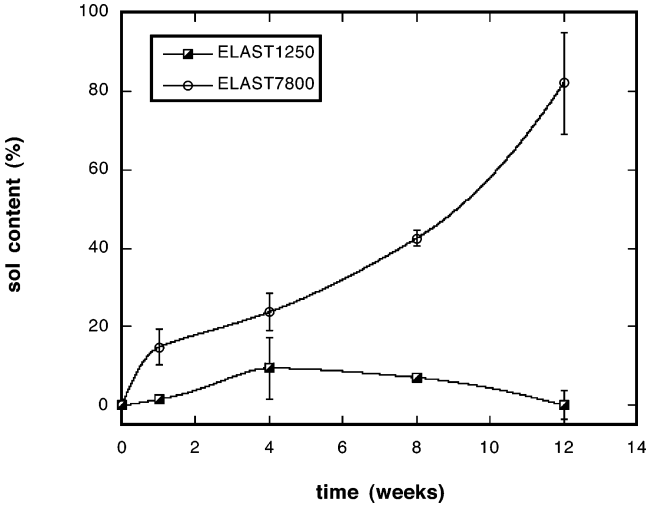

Figure 5. In vivo change in sol content during biodegradation of the elastomers.

and perhaps to a greater degree of solubility of the degradation products present at the surface in the in vivo aqueous environment. The ELAST 1250 samples degraded at a faster rate initially than the ELAST 7800 samples both in vivo and in vitro. This result is opposite that reported by Pitt et al.,[25] who observed that the degradation rate increased as the cross-link density decreased, indicating that the structure of the elastomer contributes to its degradation behavior. For both cross-link densities, the elastomers degraded slowly for the first 8 weeks, followed by an increase in both the rate and extent of mass loss. By 12 weeks, however, the two elastomer sample sets had reached the same in vivo mass loss of approximately 30% of the initial mass. The ELAST 1250 samples degraded at essentially the same rate in vivo and in vitro, as did ELAST 7800 after the first week.

The elastomers did not swell during the degradation period, but rather shrunk slightly or remained at their initial volume. This behavior was observed both in vivo and in vitro, and was not dependent on the cross-link density. This is a useful finding as it indicates that the elastomers maintain their form stability in vivo during the degradation period, a factor important for their use in drug delivery and mechanical devices.

The cross-link density also affected the sol content of the elastomers, measured during the in vivo degradation (Figure 5). While the sol content of the ELAST 7800 samples increased markedly with implantation time, reaching 82 ± 13% sol after 12 weeks in vivo, the ELAST 1250 samples exhibited little change in sol content. Thus, the ELAST 7800 samples had lost essentially the same mass as the ELAST 1250 samples by week 12; however, the remaining mass consisted of polymer chains not connected to the overall network. By contrast the ELAST 1250 samples remained a coherent network. These results demonstrate that the cross-link density of the photocured elastomer influences the mechanisms of degradation in vivo.

The mechanical properties of the elastomers (Young's modulus, E, tensile stress at break, σ, and strain at break, ϵ) were normalized with respect to their initial values (E_o, σ_o, and ϵ_o), and the change in these values in vivo are compared to their change in vitro in Figures 6−8. It should be noted that, at 12 weeks, the samples were too weak to withstand being clamped into the tensile tester. As has been reported for uncross-linked[38,46] and cross-linked[25,45] aliphatic polyesters, the mechanical properties of the elastomers decreased at the same rate and to the same extent in vivo as was observed in vitro,

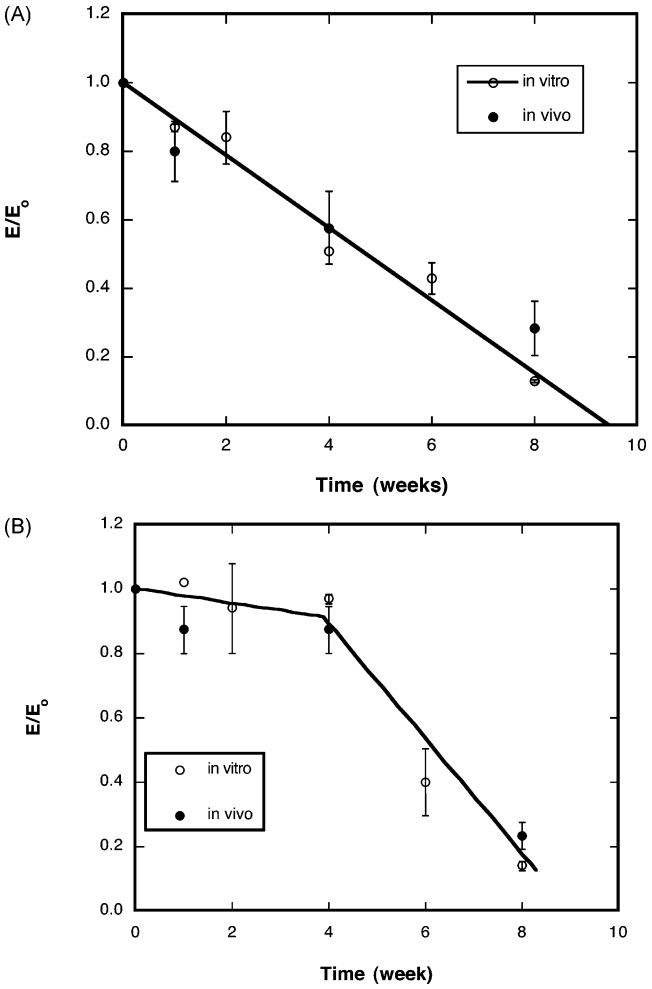

Figure 6. Comparison of the change in Young's modulus at time *t*, E_t, normalized to the initial Young modulus, E_o, with degradation time in vivo versus in vitro. The lines represent linear regressions to the data. Key: (A) ELAST 1250, (B) ELAST 7800.

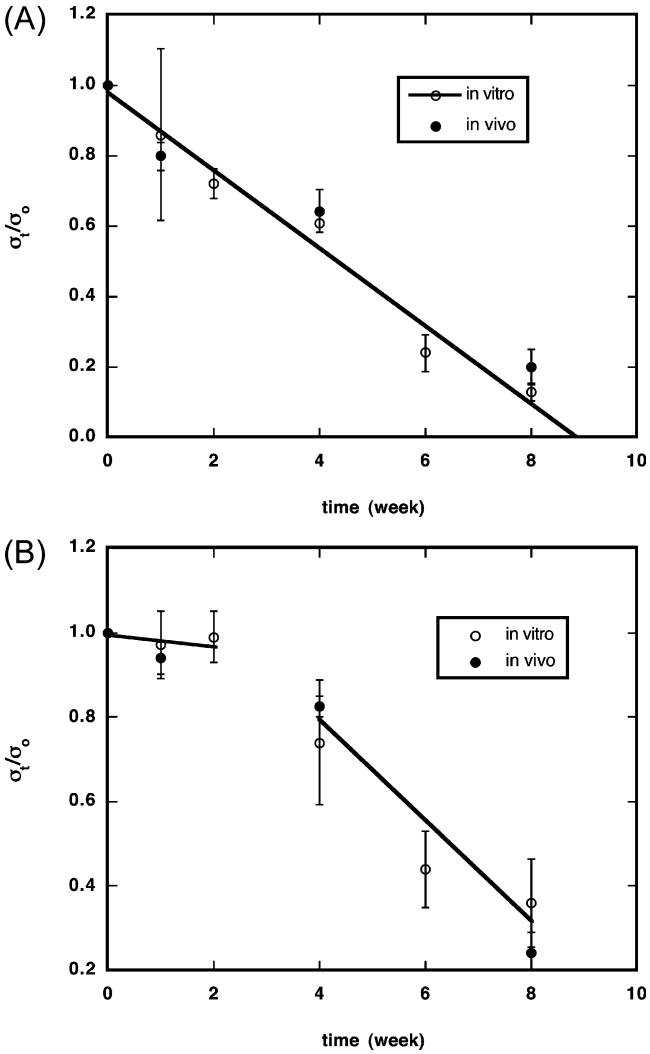

Figure 7. Comparison of the change in the stress at break at time *t*, σ_t, normalized to the initial stress at break, σ_o, with degradation time in vivo versus in vitro. The lines represent linear regressions to the data. Key: (A) ELAST 1250, (B) ELAST 7800.

while the change in property was dependent on the cross-link density of the elastomer. For the ELAST 1250 samples, E (Figure 6A) and σ (Figure 7A) decreased in a linear fashion with time (correlation coefficient, R^2, of 0.977 and 0.976, respectively), while ϵ decreased only slightly during the degradation period examined (Figure 8A). The rate constants for the decrease in E and σ were statistically equivalent (0.106 ± 0.008 and 0.110 ± 0.008 weeks^{-1}, respectively). The ELAST 7800 samples also exhibited a decrease in E and σ with time; however, for these elastomers, there was an initial induction period lasting between 2 and 4 weeks wherein Young's modulus and the stress at break decreased slowly (Figures 6B and 7B). After this period E and σ decreased markedly more rapidly, and in a linear fashion, at statistically equivalent rates of 0.163 ± 0.02 and 0.138 ± 0.02 weeks^{-1} respectively (the correlation coefficients were 0.95 and 0.956, respectively). Similarly to that of ELAST 1250, ϵ decreased only slightly during the degradation period examined (Figure 8B).

Figure 9 shows that the in vivo changes in E and σ are consistent with the changes in mass of the elastomers. Note that the in vitro data were not included in the figure, although the trends are identical. Both elastomer populations initially exhibited a linear decrease and rate of decrease in E and σ as a function of mass loss. However, while ELAST 1250 continued to exhibit a linear dependence on mass loss with time, ELAST 7800 underwent a marked decrease in tensile properties with mass loss after 4 weeks. Thus, a high cross-link density is necessary to obtain a linear strength loss with respect to mass loss with time, one of the proposed advantages of thermosets over thermoplastics.

These results are interpreted as follows. Although the implants were encapsulated by fibrous tissue in vivo, the degradation rates and changes in mechanical properties with time are essentially the same in vivo as in vitro. This result indicates that both elastomers are degrading in vivo primarily by hydrolysis at a rate determined by the extent and rate of water absorption. Due to its greater average caproyl sequence length, and its higher cross-link density, water penetration into ELAST 1250 is slower than into ELAST 7800. This results in erosion and degradation occurring more rapidly at the surface, leading to a consistent mass loss but little change in sol content with time. However, bond cleavage is occurring within the bulk, causing a decrease in Young's modulus as the number of effective elastic chains is reduced with each bond cleavage. ELAST 7800 has a more random monomer distribution, making it more hydrophilic, and a decreased cross-link density, resulting in more rapid water penetration within the elastomer. As a result, bond cleavage occurs more homogeneously initially. As acidic degradation products accumulate internally, hydrolysis becomes autocatalytic within the central portions of the elastomer, an

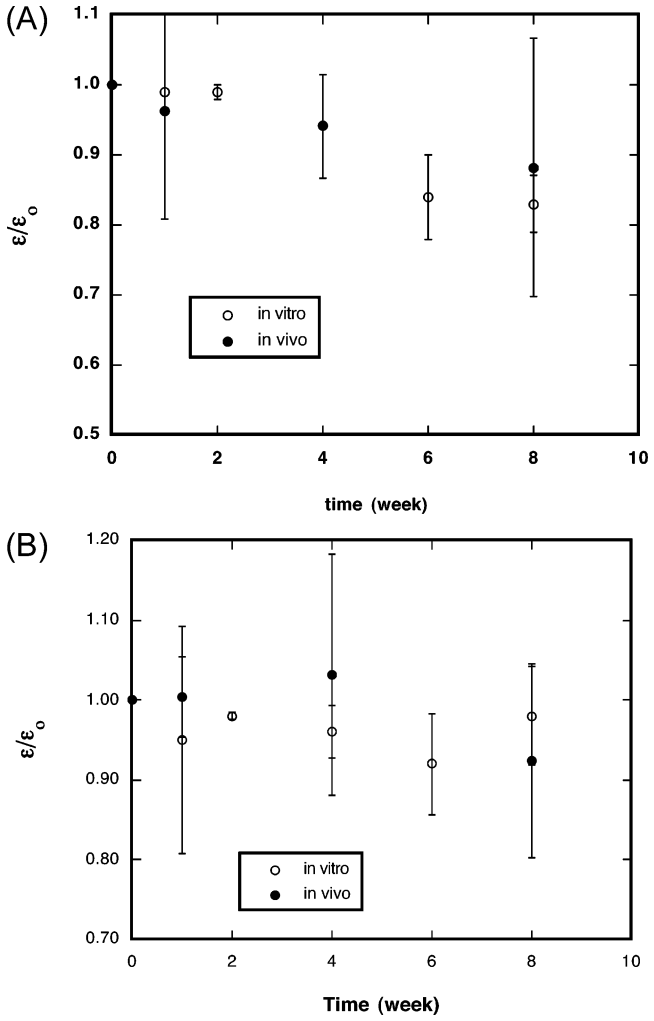

Figure 8. Comparison of the change in the strain at break at time *t*, ϵ_t, normalized to the initial strain at break, ϵ_o, with degradation time in vivo versus in vitro. Key: (A) ELAST 1250, (B) ELAST 7800.

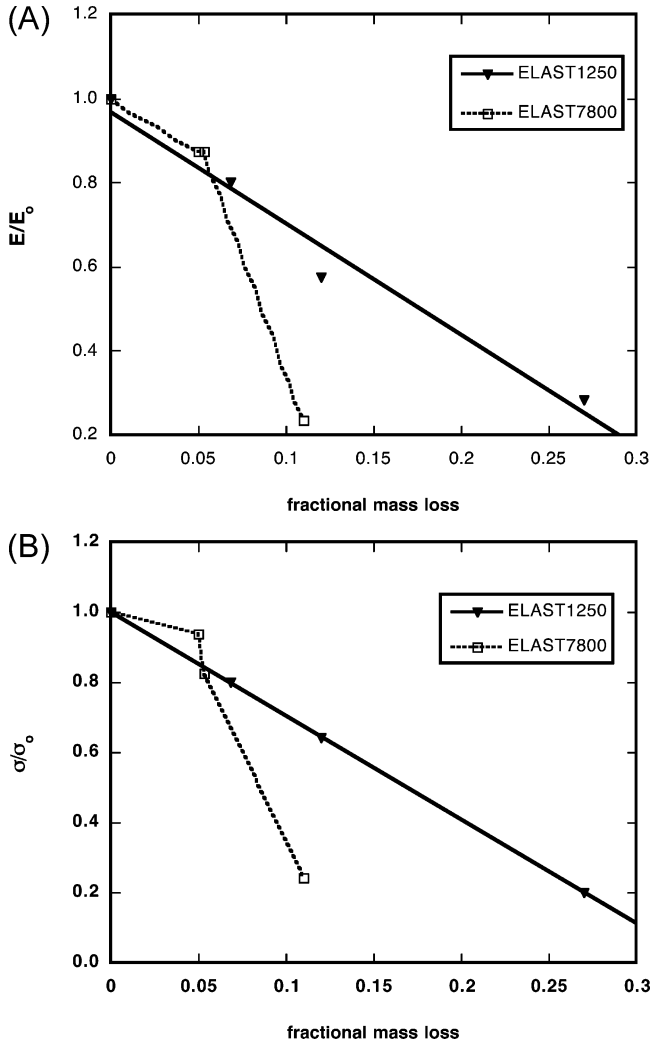

Figure 9. Normalized (A) Young's modulus and (B) stress at break versus fractional mass loss during in vivo degradation.

effect well-established for other polyesters such as poly(lactide) and poly(glycolide) in solid form.[57] This behavior is reflected in an increased sol content even though there is little observable mass loss. Young's modulus decreases only slowly because the outer layer of the elastomer has not undergone sufficient bond cleavage, and this layer provides the mechanical strength of the elastomer. The increase in mass loss and the reduced Young's modulus observed after approximately the 4 week period are due to the failure of this outer layer. This explanation is supported by our previous in vitro work, wherein a rapid decrease in internal pH to below 5 of ELAST 7800 slabs was observed after 25 days.[58] Thus, the conclusion that a linear strength change with time only occurs with high cross-link density should be tempered by recognizing that a linear strength loss with respect to mass loss for ELAST 7800 may be obtainable if the thickness of the cylinder is reduced.

The influence of mechanical stresses on enhanced degradation in vivo was also considered. The one elastomer for which enhanced in vivo degradation was observed was ELAST 7800, and the increase in mass loss was only significant over the first week. Mechanical stress on the implant can generate microcracks through which the release of soluble degradation products is made possible. However, if mechanical stresses are enhancing the mass loss, then the presence of microcracks should have produced a reduction in the stress at break with degradation. The ultimate tensile stress of ELAST 7800 remained constant until the fourth week, so mechanical stresses are not considered to have played a significant role in the degradation of the implants.

It should be noted, however, that neither the in vitro nor the in vivo degradation conditions represent a perfect sink for dissolving the polymer degradation products and removing them from the site of degradation. The compositions of the degradation products, and their solubilities in vivo and in vitro, are likely different for each elastomer as a result of their differing structure. Future work is required to determine the nature of each degradation product to determine whether dissolution and diffusion from the site of degradation play a significant role in influencing the degradation rate in vivo versus in vitro. From a practical standpoint, however, the close correlation between in vitro and in vivo degradation is useful in terms of designing devices using these materials.

Conclusions

The work presented compared the in vitro degradation behavior of elastomers prepared through the photo-cross-linking of acrylated *star*-poly(ϵ-caprolactone-*co*-D,L-lactide) to the behavior observed in vivo. The mechanical properties measured by uniaxial tension of the elastomers decrease at the same rate and to the same extent in vivo as observed in vitro. The mechanism of degradation of the elastomers was found to be

dependent on the cross-link density, which in turn is determined by the initial molecular weight of the acrylated star copolymer. For elastomers prepared from low molecular weight acrylated star copolymer (i.e., elastomers with a high cross-link density), degradation in vivo proceeded in a manner consistent with a surface erosion mechanism, while, for elastomers having a low cross-link density, degradation occurred in a manner consistent with a bulk erosion mechanism. The results demonstrate that the mechanical behavior of the elastomers in vivo can be accurately represented by in vitro degradation in phosphate-buffered saline.

Acknowledgment. This work was funded by a grant provided by the Canadian Institutes of Health Research.

References and Notes

(1) Sodian, R.; Sperling, J. S.; Martin, D. P.; Egozy, A.; Stock, U.; Mayer, J. E. J.; Vacanti, J. P. *Tissue Eng.* **2000**, *6* (2), 183−188.
(2) Alberti, C. *Minerva Urol. Nefrol.* **2000**, *52* (4), 219−222.
(3) Hinrichs, W. L.; Kuit, J.; Feil, H.; Wildevuur, C. R.; Feijen, J. *Biomaterials* **1992**, *13* (9), 585−593.
(4) Mulder, M. M.; Hitchcock, R. W.; Tresco, P. A. *J. Biomater. Sci., Polym. Ed.* **1998**, *9* (7), 731−48.
(5) de Groot, J. H.; Spaans, C. J.; Dekens, F. G.; Pennings, A. J. *Polym. Bull.* **1998**, *41*, 299−306.
(6) Gogolewski, S.; Pennings, A. J.; Lommen, E.; Wildevuur, C. R. H.; Nieuwenhuis, P. *Makromol. Chem., Rapid Commun.* **1983**, *4*, 213−219.
(7) Gogolewski, S.; Pennings, A. J. *Makromol. Chem., Rapid Commun.* **1983**, *4*, 675−680.
(8) Pitt, C. G.; Jeffcoat, A. R.; Zweidinger, R. A.; Schindler, A. *J. Biomed. Mater. Res.* **1979**, *13*, 497−507.
(9) Pitt, C. G.; Gratzl, M. M.; Jeffcoat, A. R.; Zweidinger, R.; Schindler, A. *J. Pharm. Sci.* **1979**, *68* (12), 1534−1538.
(10) Dahiyat, B. I.; Posadas, E. M.; Hirosue, S.; Hostin, E.; Leong, K. W. *React. Polym.* **1995**, *25*, 101−109.
(11) Wada, R.; Hyon, S.-H.; Nakamura, T.; Ikada, Y. *Pharm. Res.* **1991**, *8* (10), 1292−1296.
(12) Bruin, P.; Veenstra, G. J.; Nijenhuis, A. J.; Pennings, A. J. *Makromol. Chem., Rapid Commun.* **1988**, *9*, 589−594.
(13) Sinclair, R. G. Copolymers of D, L-lactide and epsilon caprolactone. U.S. Patent 4,045,418, Aug 30, 1977.
(14) Sinclair, R. G. Copolymers of L-(−)-lactide and epsilon caprolactone. U.S. Patent 4,057,537, Nov 8, 1977.
(15) Sipos, L.; Zsuga, M.; Deak, G. *Macromol. Rapid Commun.* **1995**, *16*, 935−940.
(16) Skarja, G.; Woodhouse, K. *J. Biomater. Sci., Polym. Ed.* **1998**, *9* (3), 271−295.
(17) Wang, T.; Ameer, G. A.; Sheppard, B. J.; Langer, R. *Nat. Biotechnol.* **2002**, *20*, 602−606.
(18) Kylma, J.; Seppala, J. *Macromolecules* **1997**, *30*, 2876−2882.
(19) Saad, B.; Neuenschwander, P.; Uhlschmid, G. K.; Suter, U. W. *Int. J. Biol. Macromol.* **1992**, *25*, 293−301.
(20) Grijpma, D. W.; Zondervanc, G. J.; Pennings, A. J. *Polym. Bull.* **1991**, *25*, 327−333.
(21) Bezwada, R. S.; Scopelianos, A. G. Elastomeric Medical Device. U.S. Patent 5,713,920, Feb 3, 1998.
(22) Bezwada, R. S.; Cooper, K. L. Absorbable Elastomeric Polymer. U.S. Patent 6,113,624, Sept 5, 2000.
(23) Storey, R. F.; Warren, S. C.; Allison, C. J.; Puckett, A. D. *Polymer* **1997**, *38* (26), 6295−6301.
(24) Storey, R. F.; Warren, S. C.; Allison, C. J.; Wiggins, J. S.; Puckett, A. D. *Polymer* **1993**, *34* (20), 4365−4372.
(25) Pitt, C. G.; Hendren, R. W.; Schindler, A.; Woodward, S. C. *J. Controlled Release* **1984**, *1* (1), 3−14.
(26) Palmgren, R.; Karlsson, S.; Albertsson, A.-C. *J. Polym. Sci., Part A: Polym. Chem.* **1997**, *35* (9), 1635−1649.
(27) Pogany, S. A.; Zentner, G. M. Bioerodible thermoset elastomers. U.S. Patent Sept 10, 1991.
(28) Turunen, M. P. K.; Korhonen, H.; Tuominen, J.; Seppala, J. V. *Polym. Int.* **2002**, *51*, 92−100.
(29) Storey, R. F.; Hickey, T. P. *Polymer* **1994**, *35* (4), 830−838.
(30) Amsden, B.; Misra, G.; Gu, F.; Younes, H. *Biomacromolecules* **2004**, *5* (6), 2479−2486.
(31) Gu, F.; Younes, H.; El-Kadi, A. O. S.; Neufeld, R.; Amsden, B. *J. Controlled Release* **2005**, *102*, 607−617.
(32) Perrin, D. E.; English, J. P., Polyglycolide and polylactide. In *Handbook of Biodegradable Polymers*; Domb, A. J., Kost, J., Wiseman, D. M., Eds.; Harwood Academic Publishers: Amsterdam, 1997; pp 3−27.
(33) Therin, M.; Christel, P.; Li, S. M.; Garreau, H.; Vert, M. *Biomaterials* **1992**, *13* (9), 594−600.
(34) Tracy, M. A.; Ward, K. L.; Firouzabadian, L.; Wang, Y.; Dong, N.; Qian, R.; Zhang, Y. *Biomaterials* **1999**, *20* (11), 1057−1062.
(35) Menei, P.; Daniel, V.; Monteromenei, C.; Brouillard, M.; Pouplardbarthelaix, A.; Benoit, J. P. *Biomaterials* **1993**, *14* (6), 470−478.
(36) Spenlehauer, G.; Vert, M.; Benoit, J. P.; Boddaert, A. *Biomaterials* **1989**, *10* (8), 557−563.
(37) Chegini, N.; Hay, D. L.; Vonfraunhofer, J. A.; Masterson, B. J. *J. Biomed. Mater. Res.* **1988**, *22* (1), 71−79.
(38) MainilVarlet, P.; Curtis, R.; Gogolewski, S. *J. Biomed. Mater. Res.* **1997**, *36* (3), 360−380.
(39) Matsusue, Y.; Yamamuro, T.; Oka, M.; Shikinami, Y.; Hyon, S. H.; Ikada, Y. *J. Biomed. Mater. Res.* **1992**, *26* (12), 1553−1567.
(40) van Dijk, M.; Tunc, D. C.; Smit, T. H.; Higham, P.; Burger, E. H.; Wuisman, P. I. J. M. *J. Biomed. Mater. Res.* **2002**, *63* (6), 752−759.
(41) Suuronen, R.; Pohjonen, T.; Taurio, R.; Tormala, P.; Wessman, L.; Ronkko, K.; Vainionpaa, S. *J. Mater. Sci.: Mater. Med.* **1992**, *3* (6), 426−431.
(42) Jeong, S. I.; Kim, B. S.; Lee, Y. M.; Ihn, K. J.; Kim, S. H.; Kim, Y. H. *Biomacromolecules* **2004**, *5* (4), 1303−1309.
(43) Ali, S. A. M.; Doherty, P. J.; Williams, D. F. *Biomaterials* **1994**, *15* (10), 779−785.
(44) Williams, D. F. *J. Mater. Sci.* **1982**, *17* (5), 1233−1246.
(45) Schindler, A.; Pitt, C. G. *Polym. Prepr. (Am. Chem. Soc., Div. Polym. Chem.)* **1982**, *23* (2), 111−112.
(46) Weir, N. A.; Buchanan, F. J.; Orr, J. F.; Dickson, G. R. *Proc. Inst. Mech. Eng., Part H: J. Eng. Med.* **2004**, *218* (H5), 307−319.
(47) Saikku-Backstrom, A.; Tulamo, R. M.; Pohjonen, T.; Tormala, P.; Raiha, J. E.; Rokkanen, P. *J. Mater. Sci.: Mater. Med.* **1999**, *10* (1), 1−8.
(48) Matsuda, T.; Kwon, I. K.; Kidoaki, S. *Biomacromolecules* **2004**, *5* (2), 295−305.
(49) Mizutani, M.; Matsuda, T. *Biomacromolecules* **2002**, *3*, 249−255.
(50) Helminen, A. O.; Korhonen, H.; Seppala, J. V. *Macromol. Chem. Phys.* **2002**, *203*, 2630−2639.
(51) Lang, M. D.; Wong, R. P.; Chu, C. C. *J. Polym. Sci., Part A: Polym. Chem.* **2002**, *40* (8), 1127−1141.
(52) Tsuzuki, W.; Tsuzuki, S.; Hayamizu, K.; Kobayashi, S.; Suzuki, T. *Chem. Phys. Lipids* **1995**, *76* (1), 93−102.
(53) Bero, M.; Kasperczyk, J.; Adamus, G. *Macromol. Chem. Phys.* **1993**, *194* (3), 907.
(54) Grijpma, D. W.; Pennings, A. J. *Polym. Bull.* **1991**, *25* (3), 335.
(55) Hiljanen-Vainio, M.; Karjalainen, T.; Seppala, J. *J. Appl. Polym. Sci.* **1996**, *59* (8), 1281−1288.
(56) Li, S. M.; Espartero, J. L.; Foch, P.; Vert, M. *J. Biomater. Sci., Polym. Ed.* **1996**, *8* (3), 165.
(57) Li, S. *J. Biomed. Mater. Res.* **1999**, *48*, 342−353.
(58) Gu, F.; Younes, H. M.; El-Kadi, A. O. S.; Neufeld, R. J.; Amsden, B. G. *J. Controlled Release* **2005**, *102* (3), 607.

BM050731X